GLOBAL JOURNAL OF GEOLOGICAL SCIENCES VOL. 6 NO. 2 2008: 157 - 174
 ISSN 1596 – 6798

MINERAL ASSOCIATIONS IN THE BOUSSOUMA POST BIRIMIAN MAFIC DYKE AND THEIR PETROGENETIC SIGNIFICANCE (BURKINA FASO, WEST-AFRICAN CRATON)

URBAIN WENMENGA AND JEAN LUC DEVIDAL

(Received 20 May, 2008; Revision Accepted 16 September, 2008)

ABSTRACT

A systematic electron microprobe analysis, was carried out on constituent mineral phases (olivine, pyroxene, amphibole, plagioclase, micas, opaques) in dolerite, gabbro and pegmatitic suite associated with a mafic dyke of the Boussouma area in Burkina Faso, in order to characterize the magmatic and tectonic affinity of this intrusion. The compositions and microtextures of minerals and their paragenesis led the re- examination of the magmatic origin of this dyke. The mineralogical sequence made up of ferriferous olivine, calcic- plagioclase, orthopyroxene, augite, quartz/ micropegmatite and titano-magnetite, indicates a tholeiitic composition of the parent magma of the dyke. The composition of clinopyroxenes is in agreement with tholeiitic character of this mafic dyke and typical of rocks formed by anorogenic processes in a crustal distension zone. Enrichment in quartz/ micropegmatite and in ferro- titanic oxides from the edge to the centre of the dyke and the corresponding impoverishment of olivine, are compatible with a magmatic fractionation process. The temperature of the magma during crystallization using coexistent augite and orthopyroxene geothermometry, is estimated between 1000 and 1150°C and it progressively decreased to about 600 to 800°C, during the late crystallization stages as revealed by biotite thermometry. The post magmatic evolution of the dyke is marked by the neoformation hydrothermal minerals of dominantly low temperature hydrous phases.

KEYWORDS: Dolerite, micro-analysis, minerals, tholeiite, distension, geothermometry.

INTRODUCTION

Little attention has been given to the systematic micro-characterization of mineralogical paragenesis of post Birimian mafic intrusions, which form a vast swarm in the Baoule Mossi shield within the West- African craton. Geological investigations carried out both local and regional scales on dolerite/gabbro dykes particularly, in Burkina Faso where Gamsonré (1975), P.44, Sawadogo (1983), P.42, Somda (1995), P.27 highlighted various mineral associations, but however these authors could not address to a reasonable extent, their petrogenesis, magmatic affinity and geotectonic setting. The detailed mineralogical study of Boussouma mafic dyke (Fig. A-B-C) has enabled the reconstitution of the magmatic history of this intrusion. The dyke is free of penetrative deformation or regional metamorphism, which are the major features of the Birimian hosted rocks emplaced during Eburnean orogeny (2200-2000Ma) (Castaing et al., 2003, P.24).

Geological setting

The Birimian belt of Boussouma area (Fig.1) in the Palaeoproterozoic Baoule Mossi shield (2200-2000 Ma) is cut by a basic dyke swarm among which is that of Boussouma area (Fig.1B-C), detected due to its clear aeromagnetic characteristics and geological interpretations (Paterson et al., 1985). This belt consists of dominantly greenschist volcano- sedimentary facies comprising of chemical and clastic sediments, basic and acid flows and pyroclastics. Early to late Eburnean gabbro and granite intrusions induced in these series, low grade contact metamorphism

Urbain WENMENGA, University of Ouagadougou, UFR-SVT, Department of Earth Sciences, 03 B P. 7021 Ouagadougou 03, Burkina Faso
Jean Luc DEVIDAL, Blaise PASCAL University, Laboratory "Magmas et Volcans" 5, rue Kessler, 63038 Clermont Ferrand, France.

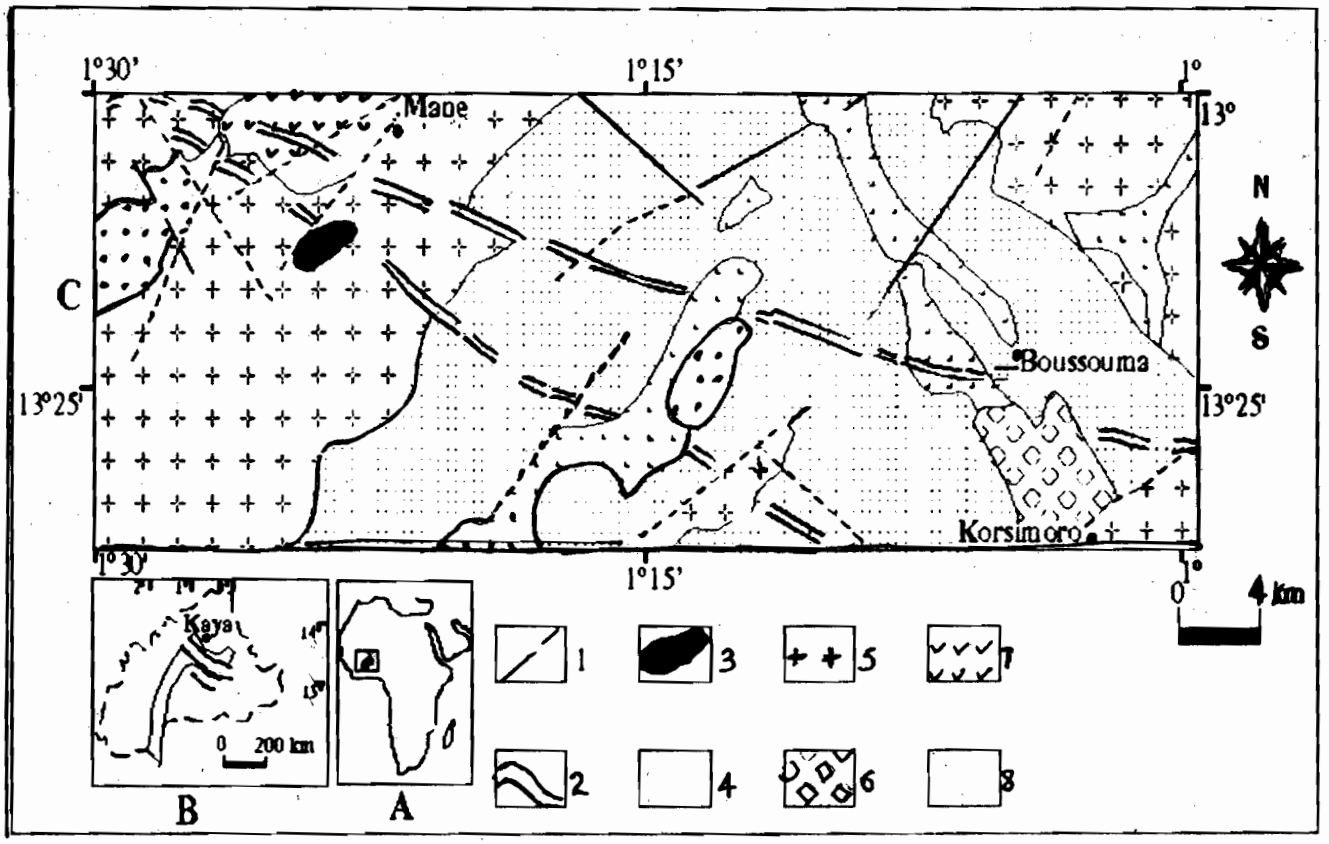

Fig. 1. A- B- C: Location (A-B) and geological map interpretation of aeromagnetic survey of Kaya- Boussouma study area (C) at 1/400.000 scale (Paterson et al.,1985)
1. Aeromagnetic fracture ; 2. Dolerite dyke ; 3. Undifferentiated basic rocks ; 4.Late gabbro intrusion ; 5. Granite ; 6. Metagabbro ; 7 Metabasalt ; 8. Birimian volcano- sedimentary series.

Analytical methods

A micro-analysis of minerals with electron microprobe Cameca SX100, was carried out in the " Magmas et Volcans " Laboratory, Blaise PASCAL University at Clermont Ferrand, France. Eight samples representing the main facies of Boussouma dyke, such as chilled (B21), fine grained (B17) and medium grained dolerite (B1, B19), coarse grained gabbro (B17", B17"') and pegmatite (B"3, B'1) were analyzed. Major and minor elements were determined on the predominant anhydrous mineral phases of which, include olivine (Table 1), pyroxenes (Tables 2, 3, 4), plagioclases (Tables 5,6,7); on the hydrous phases such as amphiboles (Tables 8,9,10), micas (Table 11) and on accessory opaque minerals (Table 12). More than one hundred analyses were performed.

Table 1: Representative chemical composition (%) of olivines from electron microprobe analysis

N° Sample	B21		B1			
N° Analysis	66	69	23	24	27	35
SiO_2	35.38	35.65	36.28	36.85	37.50	36.83
Al_2O_3	0.00	0.00	0.04	0.00	0.03	0.01
FeO	37.47	36.93	35.10	32.55	29.64	31.10
MgO	26.57	27.45	29.66	31.61	33.41	32.21
CaO	0.14	0.09	0.24	0.19	0.20	0.21
Na_2O	0.04	0.00	0.01	0.00	0.00	0.00
K_2O	0.06	0.00	0.02	0.00	0.03	0.00
TiO_2	0.06	0.17	0.11	0.00	0.00	0.05
MnO	0.45	0.50	0.45	0.40	0.37	0.50
Cr_2O_3	0.06	0.06	0.00	0.00	0.00	0.02
Total	100.24	100.84	101.92	101.60	101.19	100.94
Si	.993	.990	.987	.992	.998	.992
Al	.000	.000	.001	.000	.001	.000
Fe	.879	.858	.798	.732	.660	.700
Mg	1.112	1.136	1.202	1.268	1.326	1.293
Ca	.004	.002	.007	.005	.005	.006
Na	.002	.000	.000	.000	.000	.000
K	.002	.000	.000	.000	.001	.000
Ti	.001	.003	.002	.000	.000	.001
Mn	.010	.011	.010	.009	.008	.011
Cr	.001	.001	.000	.000	.000	.000
Total	3.006	3.004	3.010	3.007	3.001	3.006
FM	.444	.433	.402	.396	.335	.355
FO	55.53	56.65	59.78	63.09	66.49	64.50
FA	44.47	43.35	40.22	36.91	33.51	35.50

Table 2: Representative chemical composition (%) of pyroxenes from electron microprobe analysis

N° Sample	B21											B19		
N° Analysis	43	44	59	60	78	79	81	86	90	93	96	116	118	120
SiO_2	52.67	51.36	51.11	51.68	51.99	50.48	51.51	50.67	51.74	52.00	51.87	52.32	51.39	52.52
Al_2O_3	2.96	3.76	1.36	0.64	2.06	4.22	1.25	2.65	2.05	2.82	1.24	1.14	3.18	2.05
FeO	8.18	7.82	14.15	28.64	8.18	8.26	23.00	14.51	14.26	11.08	19.52	20.84	9.68	10.65
MgO	14.94	15.82	11.92	17.58	14.57	16.77	10.63	12.82	15.35	18.47	9.70	21.74	16.88	18.16
CaO	21.24	18.89	19.71	1.61	21.21	18.38	12.22	17.39	15.73	13.91	16.08	2.19	17.02	15.04
Na_2O	0.13	0.37	0.22	0.06	0.27	0.31	0.34	0.24	0.23	0.12	0.33	0.00	0.19	0.18
K_2O	0.02	0.01	0.01	0.00	0.00	0.03	0.02	0.00	0.00	0.00	0.04	0.03	0.01	0.00
TiO_2	0.40	0.53	0.37	0.19	0.46	0.47	0.32	0.92	0.56	0.39	0.18	0.44	0.46	0.28
MnO	0.23	0.19	0.41	0.53	0.19	0.22	0.60	0.38	0.44	0.29	0.56	0.44	0.29	0.29
Cr_2O_3	0.07	0.43	0.00	0.04	0.33	0.20	0.00	0.06	0.05	0.21	0.00	0.00	0.24	0.07
Total	100.85	99.18	99.26	100.97	99.26	99.35	99.88	99.63	100.42	99.29	99.52	99.15	99.34	99.24
Si	1.933	1.907	1.959	1.972	1.944	1.875	1.997	1.925	1.937	1.927	2.007	1.963	1.911	1.949
Al	0.128	0.164	0.061	0.028	0.090	184	.057	118	.904	123	.056	.050	139	.899
Fe	0.251	0.242	0.453	0.914	0.255	256	.745	461	.446	.343	631	.653	.301	.330
Mg	0.817	0.876	0.681	1.000	0.812	928	.614	725	.856	1.020	.559	1.215	.935	1.004
Ca	0.835	0.751	0.809	0.065	0.850	731	507	707	631	552	666	088	678	597
Na	0.009	0.026	0.016	0.004	0.019	.022	.025	.017	.016	.008	.024	.000	.013	013
K	0.000	0.000	0.000	0.000	0.000	.001	.000	.000	.000	.000	.002	.001	.000	000
Ti	0.001	0.014	0.010	0.005	0.013	.013	.009	.026	.015	.010	.005	.012	.012	.007
Mn	0.007	0.005	0.013	0.017	0.006	.007	.019	.012	.014	.009	.018	.013	.009	.009
Cr	0.001	0.012	0.000	0.001	0.009	.005	.000	.001	.001	.006	.000	.000	.007	.002
Total	3.995	4.002	4.006	4.009	4.001	4.027	3.977	3.996	4.009	4.001	3.972	3.999	4009	4.003
FM	0.240	0.221	0.406	0.482	0.243	.221	.554	.394	.349	.256	.537	.354	.249	.252
WO	43.71	40.06	41.36	3.29	44.18	38.07	26.90	37.12	32.39	28.69	35.54	4.47	35.25	30.79
EN	42.78	46.68	34.78	50.08	42.21	48.27	32.54	38.06	43.97	53.00	29.81	61.66	48.63	51.72
FS	13.51	13.25	23.86	46.62	13.61	13.71	40.55	24.82	23.64	18.31	34.65	33.87	16.12	17.49

Table 3. Representative chemical composition (%) of pyroxenes (continuous)

N° Sample	B19					B1							B17'''	
N° Analysis	128	129	131	136	140	20	25	26	28	30	38	102	103	104
SiO_2	53.12	51.27	52.60	51.47	53.37	50.58	52.62	52.56	51.70	52.38	50.79	50.63	51.14	51.99
Al_2O_3	0.60	2.29	1.88	3.06	1.93	0.98	1.99	2.29	1.58	2.59	2.60	2.30	2.62	2.39
FeO	23.18	14.72	13.30	11.86	19.67	30.23	14.11	11.13	22.98	14.17	13.67	15.10	13.79	10.77
MgO	20.73	15.55	17.94	15.51	23.14	15.70	19.83	17.98	21.35	20.53	14.34	14.22	13.70	15.44
CaO	1.96	14.58	13.38	17.55	1.54	1.98	10.19	15.46	1.84	9.22	16.67	16.59	17.81	19.77
Na_2O	0.02	0.25	0.15	0.21	0.00	0.04	0.25	0.25	0.01	0.10	0.23	0.20	0.16	0.44
K_2O	0.07	0.00	0.06	0.00	0.02	0.01	0.50	0.00	0.02	0.00	0.00	0.00	0.02	0.02
TiO_2	0.42	0.38	0.29	0.59	0.23	0.32	0.46	0.31	0.39	0.36	0.73	0.58	0.68	0.62
MnO	0.52	0.37	0.44	0.27	0.40	0.70	0.31	0.35	0.44	0.34	0.38	0.30	0.33	0.33
Cr_2O_3	0.02	0.08	0.00	0.11	0.01	0.01	0.06	0.08	0.00	0.13	0.00	0.00	0.00	0.07
Total	100.64	99.50	100.04	100.64	100.3	100.55	99.86	100.40	100.31	99.82	99.41	99.93	100.24	101.83
Si	1.981	1.935	1.951	1.910	1.959	1.960	1.944	1.935	1.936	1.930	1.922	1.919	1.924	1.912
Al	.026	102	.082	134	083	044	.086	.099	.069	112	115	102	116	.103
Fe	.723	464	.412	.368	.603	979	.436	.342	.720	436	432	478	434	.331
Mg	1.152	875	992	857	1.266	907	1.092	986	1.191	1.[illegible]	809	803	768	846
Ca	.078	589	531	.697	.060	.082	.403	.610	.073	[illegible]	.676	.674	718	.779
Na	.001	018	011	015	.000	002	017	.017	000	[illegible]	.017	014	.012	031
K	.003	000	002	000	.000	.000	.002	.000	000	[illegible]	.000	.000	000	000
Ti	.011	010	008	.016	.006	009	012	.008	011	[illegible]	.020	.016	019	.017
Mn	.016	.011	.013	.008	.012	.022	.009	.010	013	[illegible]	.012	.009	.010	.010
Cr	.000	.002	.000	.003	.000	000	001	002	000	[illegible]	.000	.000	.000	002
Total	3.995	4.010	4.005	4.011	3.992	4.009	4.008	4.013	4.018	4.004	4.006	4.019	4.003	4.033
FM	.390	.352	.300	.305	.327	.525	.289	.263	.381	.284	.354	.378	.366	.287
WO	3.97	30.37	27.27	36.11	3.11	4.12	20.78	31.28	3.69	18.78	35.02	34.29	37.19	39.61
EN	58.49	45.08	50.86	44.39	65.16	45.54	56.26	50.59	59.60	58.16	41.92	40.87	39.79	43.02
FS	37.54	24.55	21.87	19.50	31.72	50.34	22.96	18.13	36.70	23.06	23.05	24.85	23.02	17.36

Table 4: Representative chemical composition (%) of pyroxenes (continuous)

N° Sample	B17''17					B''3	
N° Analysis	105	106	108	112	115	27	29
SiO_2	50.91	51.17	51.05	50.47	50.54	50.89	51.17
Al_2O_3	3.35	2.78	1.95	1.79	2.37	0.21	0.05
FeO	10.08	10.29	16.55	16.64	15.30	18.31	17.06
MgO	14.02	14.33	12.89	11.99	14.40	8.35	9.11
CaO	19.94	19.60	16.84	16.80	15.26	20.66	21.49
Na_2O	0.25	0.19	0.28	0.25	0.27	0.18	0.49
K_2O	0.03	0.00	0.00	0.00	0.02	0.07	0.03
TiO_2	0.71	0.57	0.63	0.65	0.67	0.10	0.11
MnO	0.13	0.30	0.52	0.41	0.37	0.47	0.65
Cr_2O_3	0.07	0.06	0.08	0.11	0.01	0.00	0.05

Total	99.49	99.27	100.19	99.10	99.20	99.24	100.21
Si	1.909	1.924	1.933	1.946	1.925	1.998	1.986
Al	.148	.123	.087	.081	.106	.009	.002
Fe	.316	.323	.524	.536	.487	.601	.553
Mg	.783	.803	.727	.689	.818	.488	.526
Ca	.801	.789	.683	.694	.622	.869	.893
Na	.018	.013	.020	.018	.020	.013	.036
K	.001	.000	.000	.000	.000	.003	.001
Ti	.020	.016	.017	.018	.019	.002	.003
Mn	.004	.009	.016	.013	.011	.015	.021
Cr	.002	.001	.002	.003	.000	.000	.001
Total	4.004	4.004	4.013	4.001	4.012	4.002	4.027
FM	.290	.293	.426	.443	.379	.557	.521
WO	42.05	41.01	35.02	35.90	32.10	44.03	44.78
EN	41.13	41.71	37.28	35.65	42.16	24.75	26.40
FS	16.82	17.29	27.70	28.45	25.73	31.22	28.82

Table 5: Representative chemical composition (%) of plagioclases from electron microprobe analysis

N° Sample	B21										
N° Analysis	58	70	50	51	61	65	55	56	57	63	67
SiO_2	54.05	52.70	53.43	53.25	49.78	52.19	49.83	51.07	49.14	49.66	50.12
Al_2O_3	28.44	29.21	28.36	28.60	30.70	29.54	31.08	30.36	30.87	31.15	30.81
FeO	0.64	0.79	0.87	0.61	0.81	0.58	0.46	0.55	1.39	0.81	0.63
MgO	0.06	0.09	0.06	0.08	0.22	0.05	0.05	0.11	0.60	0.11	0.17
CaO	11.28	11.59	11.36	11.68	14.58	12.76	14.52	13.70	14.47	14.64	14.39
Na_2O	4.87	4.46	4.81	4.56	2.84	3.91	2.93	3.29	2.49	3.03	2.84
K_2O	0.18	0.11	0.24	0.10	0.02	0.15	0.07	0.08	0.07	0.03	0.02
TiO_2	0.04	0.00	0.05	0.04	0.01	0.03	0.00	0.10	0.03	0.00	0.06
MnO	0.00	0.03	0.04	0.06	0.03	0.11	0.00	0.05	0.04	0.00	0.01
Cr_2O_3	0.03	0.00	0.03	0.02	0.00	0.00	0.05	0.02	0.07	0.02	0.02
Total	99.59	99.09	99.25	99.00	99.00	99.32	99.00	99.34	99.17	99.44	99.06
Si	2.456	2.411	2.443	2.436	2.298	2.387	2.296	2.340	2.271	2.284	2.307
Al	1.523	1.575	1.528	1.542	1.670	1.592	1.688	1.639	1.681	1.689	1.671
Fe	.024	.030	.033	.023	.031	.022	.017	.021	.053	.031	.024
Mg	.003	.005	.004	.005	.014	.003	.003	.007	.041	.007	.011
Ca	.549	.573	.556	.572	.721	.625	.717	.672	.716	.721	.709
Na	.429	.396	.426	.404	.254	.346	.261	.292	.223	.269	.253
K	.010	.006	.013	.005	.001	.009	.004	.004	.003	.001	.001
Ti	.001	.000	.001	.001	.000	.000	.000	.003	.001	.000	.001
Mn	.000	.001	001	.002	.001	.004	.000	.002	.001	.000	.000
Cr	.001	.000	.001	.000	.000	.000	.001	.000	.002	.000	.000
Total	4.999	5.001	5.010	4.995	4.993	4.992	4.990	4.984	4.998	5.005	4.981
FM	.862	.841	.888	.829	.689	.878	.839	.753	.574	.808	.681
AB	43.41	40.57	42.75	41.17	26.02	35.34	26.62	30.14	23.66	27.17	26.29
OR	1.08	0.67	1.40	0.57	0.13	0.91	0.40	0.46	0.41	0.18	0.10
AN	55.51	58.75	55.85	58.26	73.86	63.75	72.97	69.40	75.93	72.65	73.61

Table 6: Representative chemical composition (%) of plagioclases (continuous)

N° Sample	B17	B19							B1				
N° Analysis	88	91	121	132	133	122	123	135	13	14	15	18	29
SiO_2	53.76	53.18	49.31	50.31	50.22	53.61	51.73	51.20	54.50	49.94	51.41	51.08	51.21
Al_2O_3	28.65	28.01	31.51	30.76	31.16	28.55	29.39	30.29	28.33	31.00	29.93	30.44	29.60
FeO	0.78	0.78	0.54	0.66	0.58	0.75	0.80	0.47	1.26	0.42	0.85	0.40	0.77
MgO	0.10	0.14	0.05	0.14	0.09	0.10	0.14	0.06	0.06	0.00	0.08	0.06	0.10
CaO	11.82	12.41	15.52	14.35	15.00	12.19	13.10	13.40	11.27	14.35	13.63	13.47	13.84
Na_2O	4.47	4.54	2.73	3.07	3.17	4.32	3.85	3.64	5.05	3.19	3.78	3.64	3.52
K_2O	0.10	0.08	0.03	0.00	0.00	0.05	0.06	0.00	0.13	0.09	0.09	0.04	0.05
TiO_2	0.07	0.09	0.16	0.07	0.00	0.00	0.00	0.09	0.01	0.16	0.10	0.00	0.09
MnO	0.00	0.06	0.01	0.00	0.03	6.02	0.03	0.03	0.01	0.01	0.03	0.09	0.00
Cr_2O_3	0.00	0.03	0.02	0.00	0.08	0.00	0.01	0.02	0.02	0.11	0.14	0.00	0.06
Total	99.75	99.34	99.88	99.37	100.33	99.59	99.11	99.21	100.65	99.28	100.04	99.23	99.25
Si	2.441	2.434	2.261	2.310	2.290	2.439	2.376	2.346	2.458	2.296	2.346	2.342	2.354
Al	1.533	1.511	1.703	1.664	1.674	1.531	1.591	1.636	1.506	1.680	1.610	1.645	1.603
Fe	.029	.029	.020	.025	.022	.028	.030	.018	.047	.016	.032	.003	.029
Mg	.006	.009	.003	.009	.006	.006	.009	.004	.004	.000	.005	.004	.007
Ca	.575	.608	.762	.706	.732	.594	.644	.657	.544	.707	.666	.661	.681
Na	.393	.403	.243	.272	.279	.381	.342	.323	.441	.284	.334	.323	.314
K	.005	.004	.001	.000	.000	.002	.003	.000	.007	.005	.005	.002	.003
Ti	.002	.003	.005	.002	.000	.000	.000	.003	.000	.005	.003	.000	.002
Mn	.000	.002	.000	.000	.001	.001	.001	.001	.000	.000	.001	.003	.000
Cr	.000	.001	.000	.000	.003	.000	.000	.000	.000	.004	.005	.000	.002
Total	4.988	5.009	5.003	4.991	5.010	4.986	5.000	4.992	5.011	5.000	5.011	4.997	4.998
FM	.820	.765	.859	.727	.790	.816	.765	.822	.923	.999	.862	.816	.809
AB	40.38	39.65	24.13	27.87	27.64	38.99	34.60	32.97	44.45	28.52	33.21	32.73	31.43
OR	0.58	0.46	0.18	0.00	0.00	0.28	0.36	0.00	0.73	0.55	0.55	0.26	0.32
AN	59.04	59.89	75.70	72.13	72.36	60.74	65.05	67.03	54.83	70.93	66.25	67.01	68.25

Table 7: Representative chemical composition (%) of plagioclases (continuous)

N° Sample	B17''						B''3		B'1		
N° Analysis	109	110	98	99	100	101	114	22	29	30	38
SiO_2	53.24	55.37	50.82	53.14	51.79	52.27	53.60	53.22	55.22	55.19	54.84
Al_2O_3	29.92	28.48	30.54	29.41	29.84	29.76	28.66	28.32	27.35	27.83	27.59
FeO	0.61	0.48	0.64	0.53	0.64	0.55	0.83	0.59	0.65	0.53	0.51
MgO	0.09	0.05	0.11	0.11	0.11	0.07	0.08	0.06	0.07	0.04	0.07
CaO	13.12	11.28	14.30	12.38	13.48	12.79	11.62	11.89	10.36	10.97	10.68
Na_2O	4.07	5.13	3.54	4.25	3.72	4.01	4.18	4.68	5.42	5.13	5.17
K_2O	0.07	0.10	0.00	0.08	0.02	0.11	0.09	0.02	0.09	0.09	0.09
TiO_2	0.02	0.00	0.07	0.04	0.05	0.01	0.04	0.06	0.03	0.10	0.09
MnO	0.03	0.03	0.06	0.00	0.00	0.00	0.05	0.10	0.00	0.00	0.00
Cr_2O_3	0.00	0.00	0.00	0.00	0.00	0.00	0.01	0.00	0.05	0.00	0.00
Total	101.18	100.92	100.09	99.94	99.66	99.58	99.17	99.03	99.25	99.88	99.05
Si	2.391	2.478	2.319	2.410	2.365	2.383	2.445	2.440	2.510	2.494	2.497
Al	1.583	1.502	1.643	1.572	1.606	1.599	1.541	1.527	1.465	1.482	1.480
Fe	023	.018	.024	.020	.024	.021	.031	.022	.024	.020	.019
Mg	005	.003	.007	.007	.007	.004	.005	.004	.004	.002	.004
Ca	.631	.540	.699	.601	.659	.625	.568	.583	.504	.531	.521
Na	.354	.445	.313	.374	.329	.354	.370	41.54	.478	.449	.456
K	.004	.005	.000	.004	.001	.006	.005	0.13	.005	.005	.005
Ti	.000	.000	.002	.001	.001	.000	.001	0.19	.000	.003	.003
Mn	.001	.001	.002	.000	.000	.000	.002	0.39	.000	.000	.000
Cr	.000	.000	.000	.000	.000	.000	.000	0.00	.001	.000	.000
Total	4.995	4.995	5.012	4.991	4.994	4.996	4.970	5.001	4.996	4.988	4.989
FM	.806	.859	.776	.726	.764	.811	.855	.866	.834	.889	.798
AB	35.82	44.89	30.94	38.17	33.24	35.96	39.23	41.54	48.38	45.57	46.46
OR	0.41	0.57	0.00	0.45	0.12	0.67	0.54	0.13	0.54	0.54	0.54
AN	63.77	54.55	69.06	61.38	66.63	63.36	60.23	58.33	51.08	53.90	52.99

Table 8: Representative chemical composition (%) of amphiboles from electron microprobe analysis

N° Sample	B21							B17					B19
N° Analysis	40	41	42	46	73	77	80	82	84	85	87	92	95	127
SiO_2	47.89	51.82	51.65	44.65	44.92	51.30	50.30	51.77	49.15	50.15	49.46	50.72	51.12	45.85
Al_2O_3	7.12	2.86	2.68	8.51	8.39	1.60	2.59	1.84	3.17	2.23	1.04	1.95	2.88	6.36
FeO	7.21	7.30	8.61	18.81	18.18	17.01	22.79	23.42	13.40	14.82	31.51	22.76	25.05	28.35
MgO	15.21	15.19	16.80	10.82	11.27	16.91	9.72	7.95	13.28	12.46	4.03	8.49	10.10	5.80
CaO	17.14	20.40	17.96	10.77	10.80	9.78	10.74	12.59	18.03	17.89	9.06	12.61	5.88	9.18
Na_2O	0.95	0.18	0.19	1.71	1.69	0.16	0.48	0.49	0.32	0.27	1.30	0.5	1.32	1.52
K_2O	0.04	0.00	0.00	0.38	0.34	0.01	0.04	0.05	0.03	0.00	0.20	0.06	0.05	0.36
TiO_2	1.00	0.39	0.38	1.77	1.99	0.30	0.20	0.12	0.98	0.57	0.16	0.17	0.12	1.20
MnO	0.05	0.18	0.37	0.19	0.25	0.45	0.47	0.40	0.30	0.32	1.01	0.54	0.58	0.47
Cr_2O_3	0.85	0.10	0.08	0.05	0.05	0.07	0.09	0.00	0.00	0.02	0.02	0.00	.000	0.06
OH	2.07	2.09	2.09	1.99	2.00	2.04	1.97	1.99	2.04	2.03	1.89	1.97	1.98	1.94
Total	99.54	100.51	100.80	99.66	99.89	99.63	99.40	100.61	100.70	100.89	99.68	99.78	99.09	101.11
Si	6.929	7.432	7.392	6.732	6.735	7.543	7.634	7.795	7.232	7.411	7.826	7.707	7.753	7.071
Al	1.213	.483	.452	1.511	1.483	.276	463	326	.550	.387	.193	.349	.515	1.155
Fe	.872	.875	1.030	2.372	2.279	2.091	2.893	2.949	1.648	1.826	4.169	2.893	3.177	3.656
Mg	3.281	3.248	3.584	2.432	2.518	3.705	2.198	1.783	2.913	2.737	.949	1.922	2.283	1.333
Ca	2.657	3.134	2.754	1.729	1.735	1.541	1.746	2.030	2.842	2.824	1.536	2.053	.956	1.517
Na	.266	.051	.052	.500	.491	.045	.141	.142	.091	076	398	.148	387	455
K	.007	.000	.000	.073	.065	.002	.008	009	.005	.000	040	012	009	070
Ti	.108	.041	.040	.200	.224	.033	.022	.013	.108	.062	.019	019	013	.139
Mn	.006	.022	.045	.024	.031	.055	.060	.051	.037	.039	.135	069	.075	.061
Cr	.097	.011	.008	.006	.006	.007	.011	.000	.000	.022	003	000	.000	.007
OH	1.000	1.000	1.000	1.000	1.000	1.000	1.000	1.000	1.000	1.000	1.000	1.000	1.000	1.000
Total	16.441	16.301	16.360	16.593	16.572	16.303	16.179	16.102	16.430	16.368	16.273	16.176	16.172	16.469
FM	.211	.216	.230	.496	.478	.366	.573	.627	.366	.405	.819	.606	587	.736

Table 9: Representative chemical composition (%) of amphiboles (continuous)

N° Sample	B1				B17			B13					
N° Analysis	2	19	22	33	36	107	17	18	20	21	26	28	31
SiO_2	50.57	46.83	50.90	51.05	51.96	44.45	44.95	47.28	47.05	44.84	50.92	52.43	48.69
Al_2O_3	3.30	5.76	2.47	2.30	2.24	7.49	6.48	4.30	4.06	7.00	1.42	0.59	2.86
FeO	21.66	21.45	14.72	11.42	11.03	28.01	28.76	29.73	28.53	28.75	22.33	23.33	35.05
MgO	11.31	9.68	14.19	16.23	17.22	5.71	5.26	5.66	5.62	4.90	10.44	9.59	5.19
CaO	9.56	10.28	17.78	16.11	15.04	9.50	9.51	9.67	9.21	9.86	11.70	9.77	4.67
Na_2O	0.80	1.45	0.31	0.15	0.20	1.32	1.95	1.19	1.18	1.70	0.34	0.15	0.46
K_2O	0.27	0.24	0.11	0.05	0.00	0.39	0.37	0.41	0.42	0.55	0.06	0.10	0.07
TiO_2	0.25	1.14	0.46	0.49	0.38	0.82	1.39	0.51	0.58	0.81	0.21	0.13	0.13
MnO	0.53	0.35	0.20	0.34	0.48	0.15	0.49	0.31	0.47	0.36	0.42	0.99	0.76
Cr_2O_3	0.11	0.03	0.12	0.07	0.02	0.00	0.03	0.02	0.09	0.04	0.00	0.04	0.05
OH	2.01	1.96	2.04	2.06	2.09	1.92	1.93	1.93	1.90	1.92	1.98	1.97	1.90
Total	100.36	99.18	100.30	100.27	100.66	99.76	101.12	101.02	99.10	100.73	99.83	99.09	99.84
Si	7.547	7.141	7.463	7.409	7.464	6.945	6.979	7.332	7.403	6.989	7.696	7.960	7.675
Al	.580	1.034	.426	.393	.379	1.379	1.186	.786	.753	1.286	.253	.105	.531
Fe	2.703	2.734	1.805	1.386	1.325	3.660	3.735	3.855	3.754	3.748	2.822	2.962	4.620
Mg	2.515	2.199	3.102	3.511	3.687	1.330	1.217	1.307	1.318	1.139	2.351	2.171	1.220
Ca	1.529	1.678	2.322	2.505	2.315	1.591	1.582	1.606	1.552	1.646	1.894	1.589	.788
Na	.230	.429	.880	.042	.056	.400	.587	.357	.360	.512	.099	.043	.141
K	.052	.046	.020	.008	.000	.078	.073	.081	.083	.109	.011	.019	.014
Ti	0.27	.131	.050	.053	.040	.096	.162	.050	.068	.094	.024	.015	.015
Mn	.066	.045	.024	0.41	.058	.020	.064	.041	.062	.047	.053	.127	.101
Cr	.013	.003	.014	.007	.002	.000	.004	.003	.010	.005	.000	.048	.006
OH	1.000	1.000	1.000	1.000	1.000	1.000	1.000	1.000	1.000	1.000	1.000	1.000	1.000
Total	16.267	16.445	16.317	16.360	16.330	16.504	16.592	16.431	16.366	16.579	16.206	15.999	16.116
FM	.524	.559	.371	.289	.273	.734	.757	.748	.743	.769	.550	.587	.794

Table 10: Representative chemical composition (%) of amphiboles (continuous)

N° Sample	B1							
N° Analysis	21	22	25	27	31	32	33	36
SiO_2	51.17	44.28	44.07	50.88	48.30	48.91	51.92	44.05
Al_2O_3	2.02	7.15	7.15	2.50	6.51	6.67	1.23	6.23
FeO	27.35	28.10	27.41	27.12	15.02	14.49	8.62	28.67
MgO	8.88	5.44	5.64	9.24	13.79	13.95	13.92	5.56
CaO	6.37	9.56	9.34	7.39	10.77	10.68	22.54	9.20
Na_2O	0.37	1.78	2.03	0.39	1.19	1.05	0.09	1.63
K_2O	0.06	0.18	0.18	0.07	0.26	0.20	0.01	0.31
TiO_2	0.29	1.79	1.69	0.31	1.20	0.77	0.35	1.47
MnO	0.56	0.52	0.30	0.57	0.21	0.33	0.29	0.35
Cr_2O	0.01	000	0.03	0.08	0.08	0.03	0.00	0.02
OH	1.96	1.93	1.91	1.98	2.03	2.04	2.07	1.90
Total	99.05	100.72	99.75	100.51	99.36	99.11	101.04	99.39
Si	7.836	6.880	6.893	7.698	7.113	7.183	7.510	6.961
Al	364	1.309	1.319	445	1.129	1.155	210	1.160
Fe	3.502	3.651	3.586	3.431	1.850	1.780	1.042	3.789
Mg	2.027	1.259	1.314	2.083	3.026	3.055	3.001	1.308
Ca	1.045	1.590	1.564	1.197	1.699	1.680	3.494	1.557
Na	.110	535	614	113	340	297	025	497
K	011	034	036	012	048	038	002	063
Ti	033	208	198	035	132	084	037	174
Mn	073	067	039	072	026	040	035	047
Cr	001	000	004	009	009	003	000	002
OH	1.000	1.000	1.000	1.000	1.000	1.000	1.000	1.000
Total	16.006	16.539	16.570	16.100	16.377	16.319	16.358	16.561
FM	638	747	734	627	382	373	264	745

Table 11: Representative chemical composition (%) of micas from electron microprobe analysis

Mineral	Chlorite				Biotite	
N° Sample	B1		B19		B1	B1
N° Analysis	34	35	125	126	41	37
SiO_2	27.10	27.50	33.66	35.33	35.12	33.51
Al_2O_3	17.44	17.73	13.92	13.13	12.69	13.53
FeO	33.99	31.63	32.13	31.81	31.22	31.63
MgO	9.00	11.60	3.60	4.67	4.61	6.16
CaO	0.19	0.21	0.03	0.24	0.22	0.29
Na_2O	0.02	0.00	0.21	0.57	0.24	0.12
K_2O	0.05	0.00	8.96	8.08	8.12	5.40
TiO_2	0.07	0.12	4.02	3.48	3.56	4.34
MnO	0.24	0.15	0.16	0.16	0.20	0.11
Cr_2O_3	0.05	0.03	0.00	0.06	0.01	0.00

OH	10.91	11.18	3.71	3.78	3.73	3.73
Total	99.07	100.16	100.40	101.31	99.71	98.83
Si	5.951	5.893	5.432	5.598	5.645	5.378
Al	4.514	4.478	2.648	2.452	2.405	2.558
Fe	6.241	5.667	4.336	4.215	4.197	4.245
Mg	2.946	3.703	.867	1.102	1.105	1.473
Ca	.044	.048	.006	.041	.037	.050
Na	.009	.000	.065	.173	.073	.036
K	.014	.000	1.843	1.632	1.666	1.106
Ti	.010	.019	.487	.414	.430	.524
Mn	.044	.027	.022	.020	.026	.014
Cr	.008	.005	.000	.007	.001	.000
OH	8.000	8.000	2.000	2.000	2.000	2.000
Total	27.786	27.843	17.709	17.659	17.589	17.388
FM	.680	.605	.834	.793	.792	.743

Table 12: Representative chemical composition (%) of oxides from electron microprobe analysis

N° Sample	B19	B'1
N° Analysis	138	39
SiO_2	0.02	0.00
Al_2O_3	0.05	0.00
FeO	42.46	42.72
Fe_2O_3	6.56	4.52
MgO	0.13	0.02
CaO	0.06	0.06
Na_2O	0.07	0.06
K_2O	0.00	0.04
TiO_2	49.04	50.36
MnO	1.43	2.50
Cr_2O_3	0.00	0.00
Total	99.82	100.28
Si	.001	.000
Al	.003	.000
Fe	1.800	1.803
Fe	.250	.171
Mg	.009	.001
Ca	.003	.003
Na	.007	.006
K	.000	.002
Ti	1.869	1.911
Mn	.061	.106
Cr	.000	.000
Total	4.005	4.006
FM	.994	.999

Petrography

The dyke occurs as boulders of variable sizes and enclosing Birimian xenolith rocks. It also caused volcanic chilled margins at the contact with Eburnean granitic and volcano-sedimentary country rocks. From the margin to the centre of the dyke, appears a petrographic suite made up sequentially of chilled dolerite, dolerite (ss), gabbro, pegmatite and locally graphic micropegmatite. Within the group of dolerite and gabbro bodies which form the essential rocks of the dyke, there appears to be progressive and regular grain variations (fine, medium, coarse). Elsewhere, many authors (Ross, 1983, P.1120, Bertrand, 1987, P.118, Potdevin et al., 1994, P.251, Napon, 1988, P.36) have reported textural grain changes between the core and the margin of dolerite dykes. Under the microscope, the chilled dolerites are composed of pyroxene glomero-porphyritic or olivine and plagioclase with porphyritic texture, while in the group of dolerite/gabbro suite, coexist intergranular, ophitic and intersertal textures. In these major suites, the plagioclase phases are commonly embedded by interstitial pyroxenes and could be described as local adcumulate and orthocumulate microtextures in the gabbro as in the Neoproterozoic basic dykes of Igherm inlier (El Aouli et al., 2001, P.372). Their preferential orientation indicates fluidal or igneous lamination structures (Bickford, 1963, P.227, Rivers and Mengel, 1988, P.1630) frequent in layered intrusions (Pons, 1982, P.81). Similar petrographic differentiations were described in numerous mafic sills and dykes of various age throughout the world (Vicat et Pouclet, 1995, P.358, Hafid, 1992, P.112, Machairas, 1975, P.195, Cadman and Tarney, 1990, P.19). These observations are interpreted as the consequence of the variation of the cooling rate during magmatic emplacement (Machairas, 1975, P. 195, Vicat et Vellutini, 1987, P.62, Azambre et al., 1987, P.382, Sutcliffe, 1989, P.69). The optical features and the microtextural relationships in these rocks enable their categorization into three groups, (i) a primary anhydrous minerals group (olivine, pyroxene, plagioclase, quartz, opaques), (ii) a group of late magmatic hydrous phases (amphiboles, micas) related to local volatil enrichment (Rathna and al., 2000, P.405) and (iii) a group of secondary post magmatic phases (phyllites, carbonates, epidote, iron oxides).

Characterization of mineral associations

Primary anhydrous minerals

Olivine

In the fine or medium grained dolerites, olivine crystals are strongly corroded by plagioclase and pyroxene (Fig.2-1) or form globular inclusions in clinopyroxenes. The coexistence of quartz and olivine in some samples, may be due to a crustal contamination or hybridization of the parent magma (Botha and Hodgson, 1976). In the chilled dolerite, olivine forms euhedral or anhedral phenocrysts with etching pit filled by the mesostasis or gaps occupied by augite crystals. Coronas of magnetite and orthopyroxene spread out around these phenocrysts due to olivine and residual liquid reaction. For this purpose, the following reaction was proposed by Pons (1982, P.119).

$(Mg, Fe)_2 SiO_4 + SiO_2 = 2 [(Fe, Mg) SiO_3]$

olivine + liquid= orthopyroxene. In other dykes, olivine exhibits continuous clinopyroxene rim and is restricted to dolerite suite. The corona microtexture is interpreted as a consequence of slow cooling of the parent basic magma of the dyke (Rathna and al., 2000 P.406). The content of olivine decreases from 5% to 1% from chilled dolerites to interior gabbros and is absent in the pegmatites and micropegmatite suites. Olivine composition corresponds to a hyalosiderite (Fo: 55.3-66.49) (Table 1).

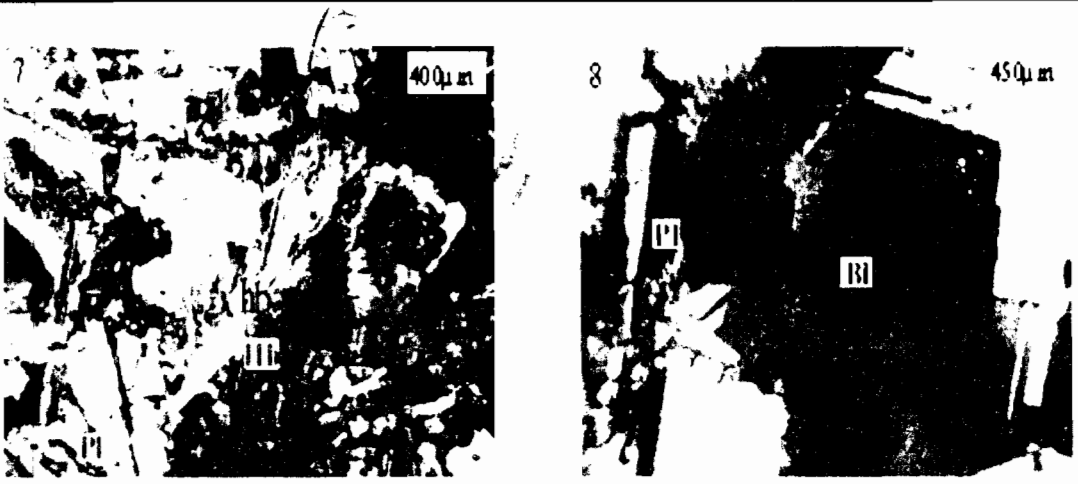

Fig. 2: Photomicrographs
1- Medium grained dolerite consisting of subhedral plagioclase (Pl), interstitial augite and strongly corroded anhedral olivine (Ol); 2. Ophitic and intergranular texture of coarse grained gabbro spaces between tabular crystals of plagioclase (Pl) are filled by poecilitic clinopyroxene (cpx). 3. Large crystal of clinopyroxene (augite) enclosing numerous plagioclase microlites in dolerite/ gabbro. 4. Aggregate of vermicular symplectite pyroxene crysts in the fine grained dolerite. 5. Photomicrograph illustrating accumulation of plagioclase microlites around poikilitic augite in chilled dolerite. 6. Cumulus phases of elongate plagioclase crystals displaying igneous lamination structure, in a medium grained dolerite. Ilmenite (dark crysts) is post cumulus phase. 7. Sheef- like texture of late fibrous greenish hornblende (Hb) in medium grained dolerite. 8. Large lamellar biotite (Bi) and iron oxide replacing uralites between spaces of plagioclase crystals.

Pyroxenes

Dominant clinopyroxenes and subordinate orthopyroxenes together with plagioclase, represent the most abundant phases of dolerite and gabbro constituting the dyke. The clinopyroxenes occur as irregular anhedral crystals, interstitial to plagioclase. (Fig.2-2). They are enclosed within the microlites of plagioclases (Fig.2-3) and constitute common prevalent species of all the suite. The orthopyroxenes generally form inclusions in clinopyroxenes or cluster of crystals with symplectite texture (Fig.2-4) developed at their contact with plagioclase or with the other types of pyroxene. This type of microtexture is interpreted as the product of exsolution reaction by atomic diffusion as the case of myrmekites (Mongkoltip and Ashworth, 1983, P.637). Frequent exsolution granules, discrete zoning and rare twins are associated with clinopyroxenes. The orthopyroxenes are of hypersthene composition, while clinopyroxenes display an important range of composition (Tables 2 to 4) evolving from calcic-subcalcic to ferriferous augites (Fig.3). Fe rich augites characterize the more differentiated suite of the dyke (Gabbro, pegmatite) and are attributable to magmatic fractionation (Reid, 1990, P.328). The absence of Ca-poor clinopyroxene such as pigeonite in this dyke, is due to the high water content in the magma (Pons, 1982, P.142).

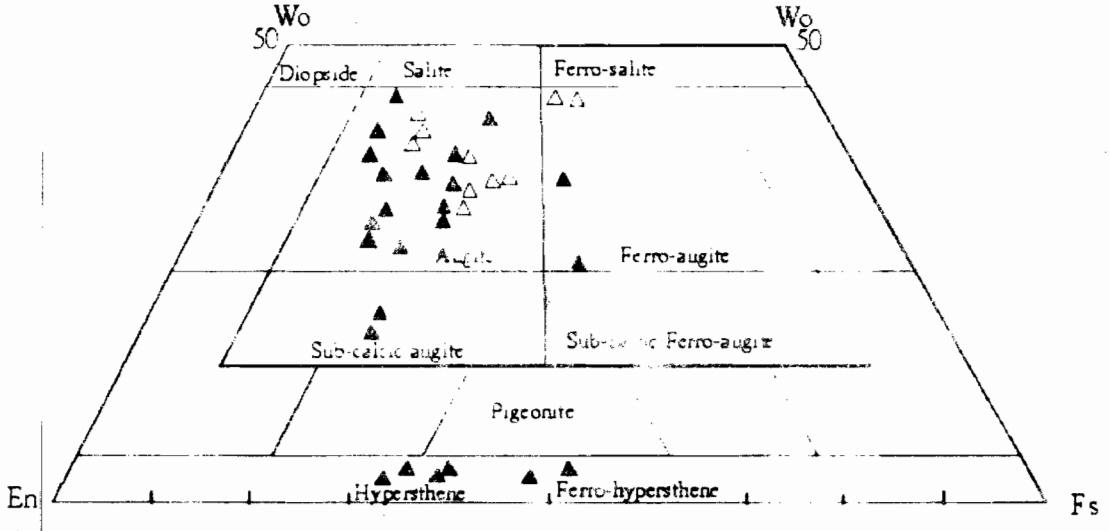

Fig. 3: Plot of pyroxene composition of representative rock samples of Boussouma dyke in Wo- En- Fs diagram (Poldervaart and Hess, 1951). Full triangle : pyroxene of dolerites ; empty triangle : pyroxene of gabbros and pegmatites.

Plagioclases

Plagioclases are the predominant minerals constituent (30 to 40%) of the various suite of the dyke and occur as tabular subhedral to euhedral crystals of increasing size from chilled dolerites to pegmatite or as laths ophitically inter- grow with pyroxenes (Fig 2-3). Plagioclase phenocrysts are confined to chilled dolerite displaying frequent gaps filled with augite crystals, but absent in

the core of the dyke. This observation is best explained by differentiation by a rapid quenchy magma rather than by flow differentiation (Ross, 1986, P.234). The accumulation of basic plagioclase microlites of mesostasis around mafic phenocrysts, suggests an emplacement in the country rocks of the magma still in molten stage (Fig.2-5). However, the massive accumulation of tabular or stubby crystals types in the medium or coarse- grained suites (Fig.2-6) rather suggests an earlier crystallization in the magmatic chamber. Plagioclase composition varies from labradorite to bytownite, irrespective of conditions of formation or that of host facies (Fig.4). These plagioclases contain high percentage of iron (0.40 to 1.39%) (Tables 5 to 7) relative to those of the Triassic "ophites" of Pyrenean field (Azambre et al., 1987, P.390).

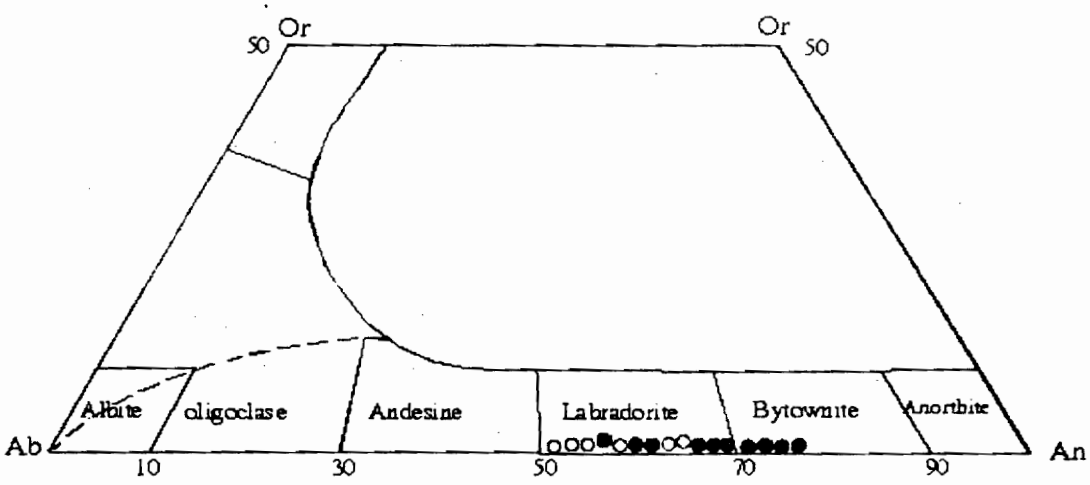

Figure 4. Labradorite to bytownite composition of feldspar in Or- Ab- An diagram Full circle : plagioclase of dolerites , empty circle : plagioclase of gabbros and pegmatites.

Quartz

The late crystallization of quartz is explained by its occurrence as interstitial and poecilitic minerals which must have crystallized after the opaque oxides. Its content is less than 5% in dolerite/gabbro, but increases within the pegmatite (10%) and the graphic micropegmatitic suite (60%), which could represent an eutectic crystallization products of the residual liquid (Somda, 1995, P.27, Gamsonre, 1975, P.70, Azambre et al., 1987, Hafid, 1992, P.116, Napon, 1988, P.37).

Opaque minerals

They are omnipresent minor components of all the suite of the dyke. Their proportion particularly increases (5 to 10%) in the gabbro and in the pegmatite bodies. They resemble inter-cumulus phases (Fig.2-6) of plagioclase, formed interstitial phases or as a result of symplectitic intergrowth with brownish hornblende. Some opaque oxides were developed as magmatic exsolution or oxidation products of mafic minerals. Their composition corresponds to ilmenites (Table 12) with relatively high ratio of MnO (1.43 to 2.5%) resulting from the major substitution of Fe-Mn in the lattice of the minerals (Reynolds, 1983, P.218). The development of biotite rim around opaques can be explained by the reaction between oxide phases and the residual liquid (Reynolds, 1983, P.218)

Accessory minerals

Zircon and sphene are rare in the dolerite body, while apatite forms euhedral prisms in the gabbros, pegmatites and micropegmatites bodies. The crystallization of this type of apatite described in some basic dykes, could result from a magma enriched in phosphorus, fluorine and probably chlorine (Hafid, 1992, P.137, Azambre et al., 1987, P.391) .

Late magmatic hydrous minerals

Amphibole

The abundance of amphiboles depends on the intensity of the transformation of clinopyroxene in the rock. Their color variation is used to distinguich two families of amphiboles in each body of the dyke; brownish amphiboles and the greenish amphiboles (Fig. 2-7). The first family may be magmatic, while the second could be derived from clinopyroxenes uralitization or from the successive alterations of uralites (Fig.2-7). The brownish amphiboles are distinguished from the other types by their enrichment in TiO_2 (1.14 to 1.99%) and in alkalis (1.45 to 2.32%) (Tables 8 to 10). They display a magnesio-hornblende composition similar to amphiboles of the Sirba valley dolerite dykes in Niger (Ama Salah, 1991, P.204) whereas the greenish amphiboles are related to actinolite and actinolitic hornblende (Fig.5) based on the classification of Leake, (1978). The amphibole composition has been reported in the Marocan Proterozoic dolerites (Hafid, 1992, P.120). Other types of classification suggest the brownish amphiboles formed ealier and is of ferro- edenite composition (Hafid, 1992, P.121) of pargasite (Pons, 1982, P.163, Pemberton and Offler, 1985, P 593) or of pargasitic hornblende (Fabries et al., 1984, P.731). The diagram Ti versus Si of Leake, (1965) (Fig.6) is not in conformity with the grouping of the amphibole into igneous brownish to the secondary or " metamorphic " greenish types. It seems that the color distinction of these two groups of amphiboles, reflects their chemical composition and the thermal condition of magmatic crystallization rather than a difference of metamorphic grade. All the amphiboles may be of magmatic to hydrothermal origin (Fonteilles et Muffat, 1970, P.557) The crystallization of two groups of amphiboles, implies

the presence in the residual liquids of abundant water (Pons, 1982, P.217) or deuteric fluids (Fonteilles et Muffat, 1970, P.557) permitting for continuous retrograde reactions. The distribution of Mg and Fe in these various types of amphiboles as manifested by the individual body, suggests a negative correlation between these elements (Fig.7). The behavior of these two elements in the amphiboles, is due to a ferro-magnesian substitution during magmatic cooling (Hafid, 1992, P.128).

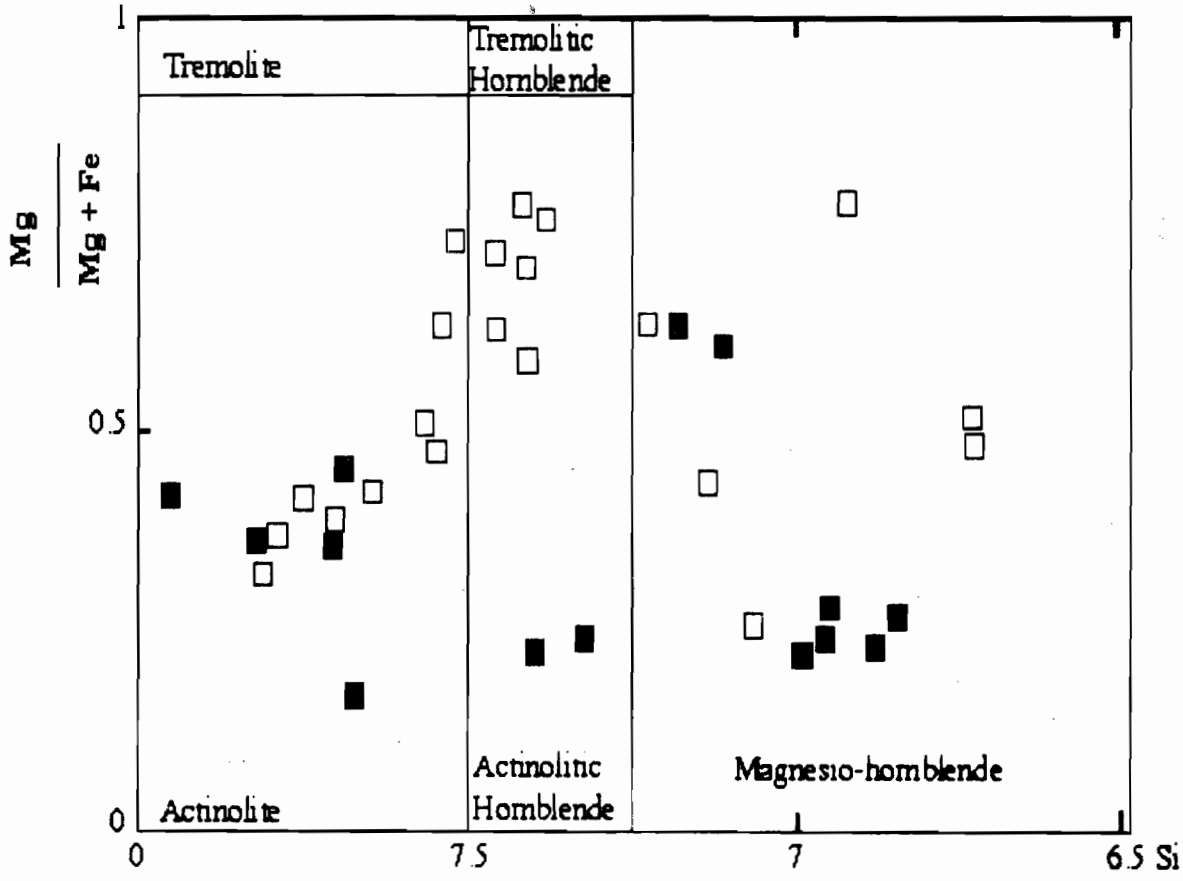

Figure 5. Classification diagram after Leake, (1978) showing various composition of amphiboles in the main facies of Boussouma dyke. Empty square : amphibole of dolerites., full square : amphibole of gabbros and pegmatites.

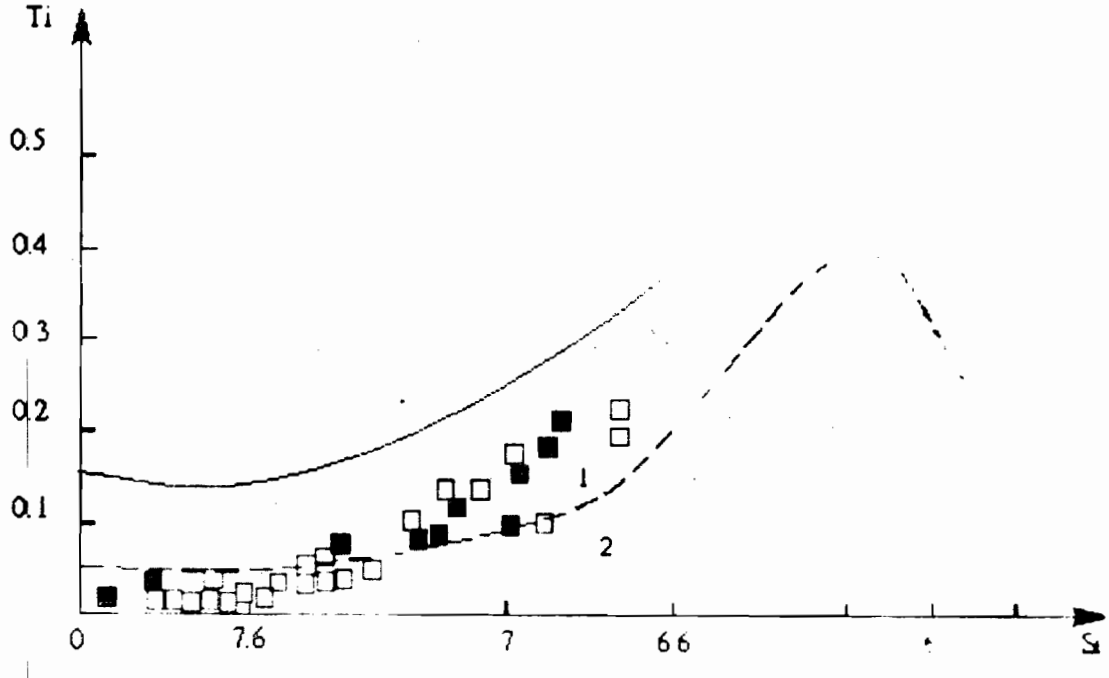

Figure 6: Plot in Ti- Si diagram (Leake, 1965) of amphiboles composition, pointing to igneous and metamorphic origin. 1. Magmatic amphiboles field ; 2. "Metamorphic amphibole" field. Same legend as figure 5.

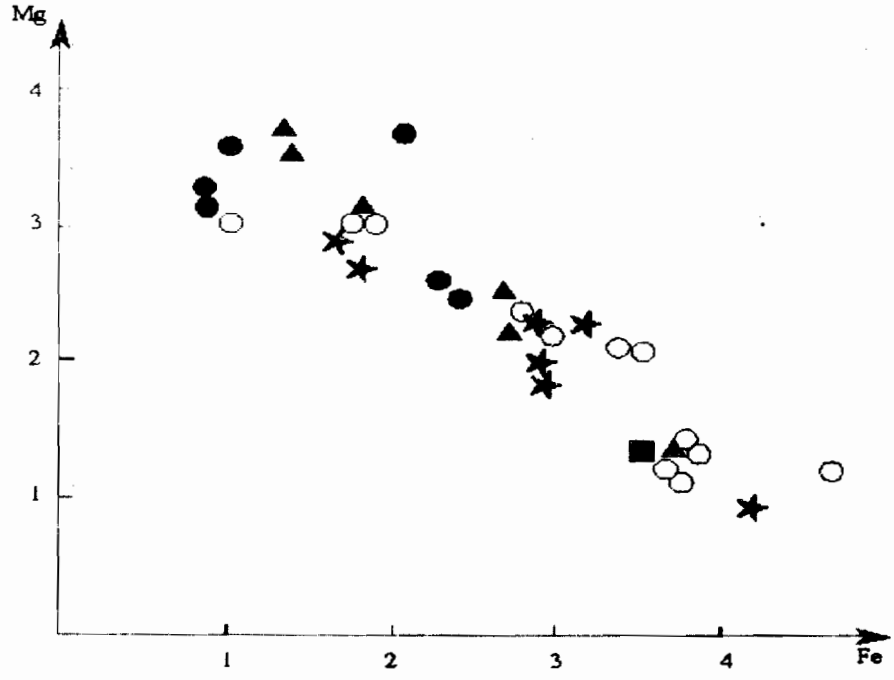

Figure 7: Chemical covariation of Mg versus Fe in amphibole minerals in the main facies of Boussouma dyke. Full circle : amphiboles of chilled dolerite ; full star : amphiboles of fine grained dolerite ; full triangle : amphiboles of medium- grained dolerite ; full square: amphiboles of gabbros ; empty circle : amphiboles of pegmatites.

Micas

Ti-rich biotite (3.5 to 4.5% TiO_2) (Table 11) in this dyke is a minor constituent showing lepidomelane composition (Fig.8). It partially replaces or pseudomorphoses with secondary iron oxide exsolution (Fig.2-8), actinolite or actinolitic hornblende minerals. Symplectitic intergrowth between biotite, opaques and amphiboles are frequent in the majority of the facies. In the sequence of retrograde transformation of the amphibole minerals, which is accompanied by systematic iron oxide exsoluion, biotite appears belatedly in the following mineral reactions: magnesio-hornblende → actinolitic- hornblende→ actinolite→ biotite→ chlorite. The cryptocrystalline chlorite which enhances intersertal texture of more altered gabbro and dolerite, is identified as brunsvigite (Hey, 1954) (Fig.9) (Table 11). The coexistence of lamellar brown biotite and brown amphibole suggests a late magmatic crystallization of these micas under moderately high temperature conditions and hydrostatic pressure (Ama Salah, 1991, PP.204-211, Azambre et al., 1987, P.392, Fabries and al., 1984, P.731, Cadman and al., 1990., P.18, Pemberton and Offler, 1985, P.596, Airo, 1999, PP.897-899).

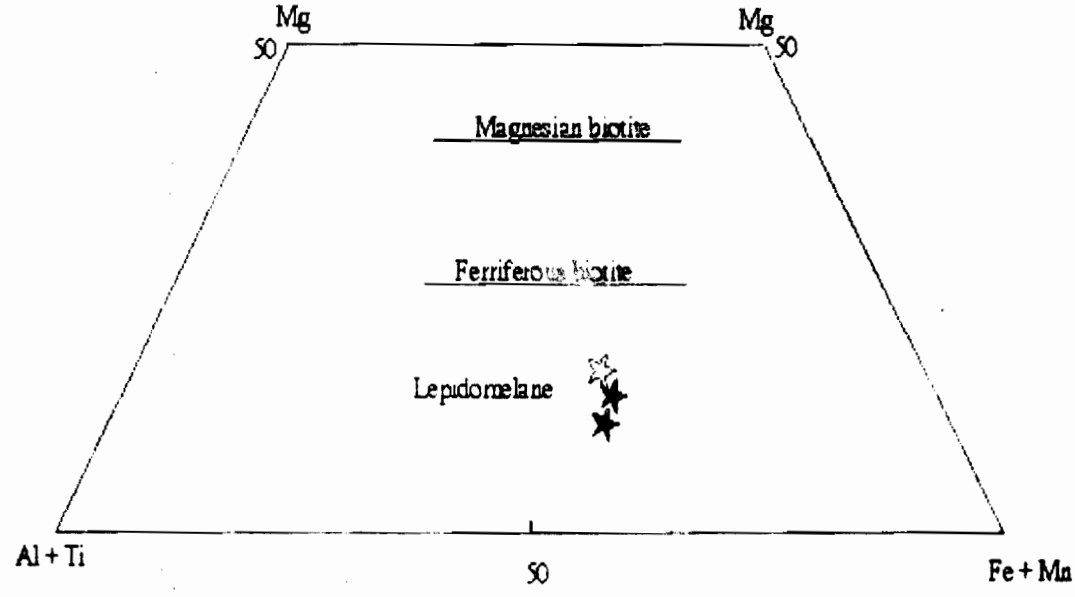

Figure 8: Lepidomelane composition of biotites plotted in Foster (1960) micas classification diagram. Full star : medium grained dolerite , empty star : pegmatites.

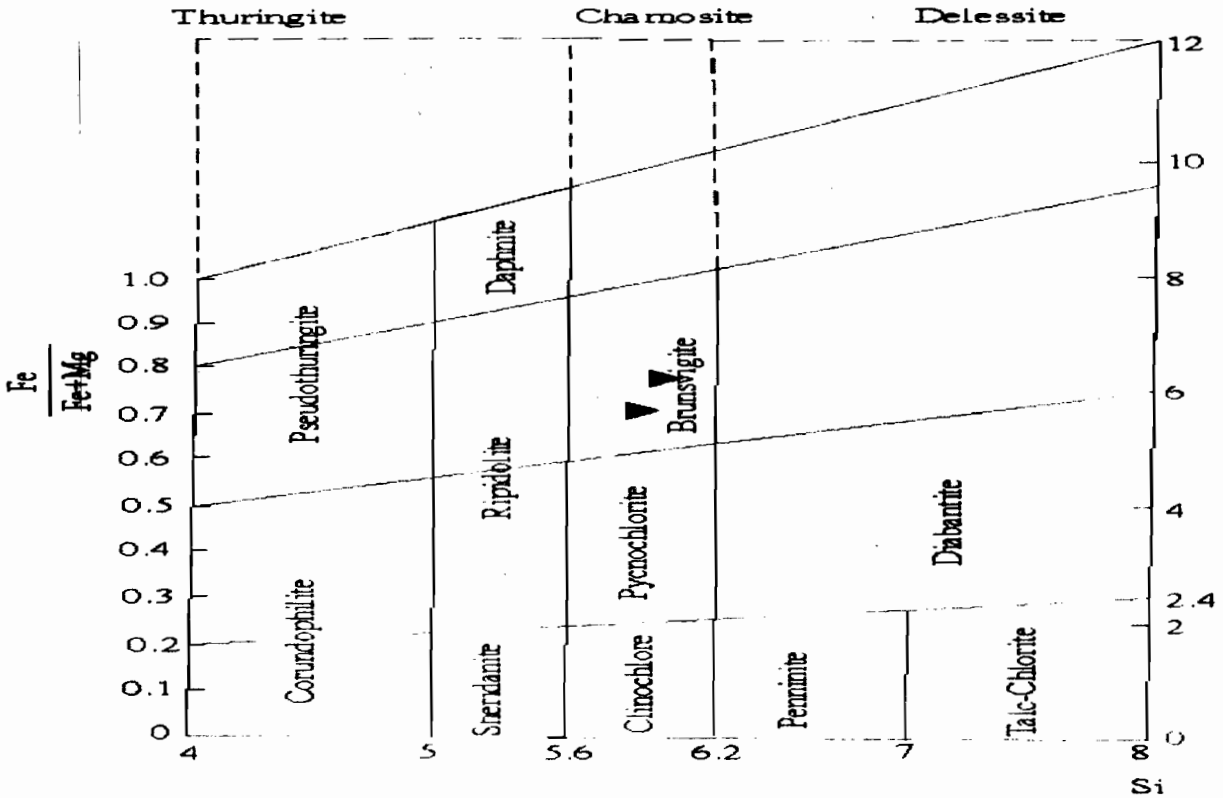

Figure 9: Brunsvigite composition of chlorites from pegmatite samples in the (Fe/Fe +Mg)-Si diagram (Hey, 1954).

Post magmatic hydrothermal minerals

The action of the hydrothermal fluids in the plastic strain rocks (undulating quartz, flexure of pyroxenes, mechanical twinnings of plagioclase) or the cracked or cataclastic bodies, consequently generates a neo-formation of a wide spectrum of dominant hydrous and subordinate anhydrous minerals. The cracks of primary minerals of some microfractured rocks serve as preferential drains for the circulation of fluids (Azambre et al., 1987, P.380). In the dyke, these bodies display perthitic and sericitic microtextures of plagioclase suggesting a formation during intense alteration; biotite flakes, epidote, carbonate, chlorite as filling the cracks of pyroxenes or amphiboles, actinolite in those of plagioclases are products of hydrothermal origin. Olivine is partially replaced by an aggregate of serpentine and chlorite or pseudomorphosed into serpentine and small brown hornblende. Talc is less frequent in the alteration products of tremolite/actinolite The skeletal or grid iron oxides are formed at the expense of leucoxene

Petrogenetic interpretation

The use of the composition of clinopyroxene phenocrysts to characterize the magmas affinities and the geotectonic settings of recent volcanic or paleovolcanic series, was introduced with previous works of Letterrier and al. (1982, P.140) and of Molard et al. (1983 P 903). Plots of the compositions of clinopyroxene extended from the dolerites and gabbros/pegmatites in Al versus Si diagram (Fig 10) show their non- alkaline affinity

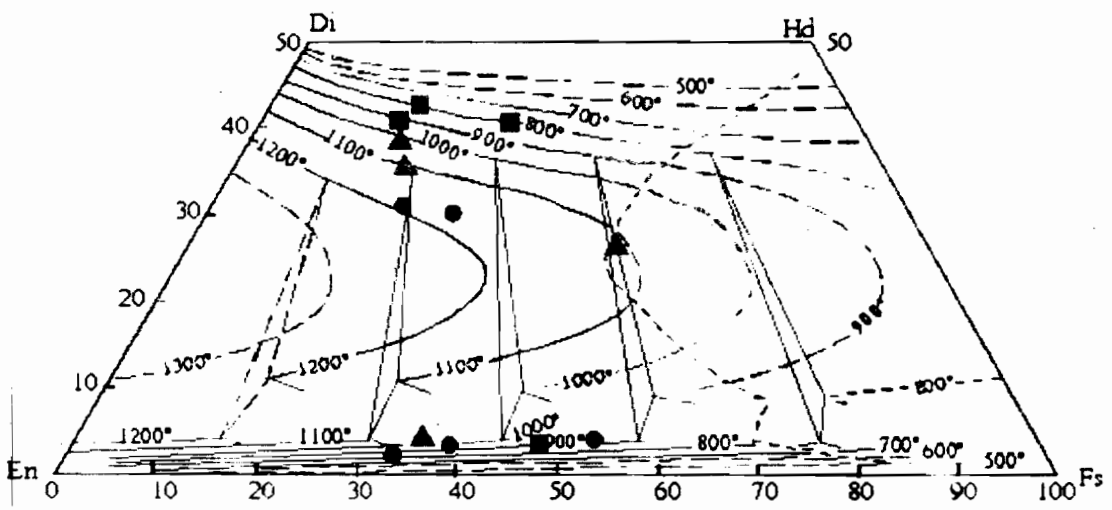

Figure 10: Alt versus Si diagram (Kushiro, 1960) showing non alkaline composition of clinopyroxene in the Boussouma dyke. Full triangle : dolerite; empty triangle : gabbros and pegmatites.

Those of dolerites are mainly tholeiitic basalt in composition (Fig.11), while clinopyroxenes of coarse - grained gabbro, plotted in calc- alkaline but remain nevertheless in the statistical overlap field of tholeiites. The over all mineralogical characteristics of the dyke attests to its tholeiitic affinity, especially due to the presence of ferriferous olivine (Ama Salah, 1991, P.195), augite, hypersthene, calcic- plagioclase, iron oxides, quartz and micropegmatite (Vicat et Pouclet, 1995, P.358, Fonteilles et Muffat, 1970, P.568, Ama Salah,1991, P.194, Fodor and al., 1972, Poidevin, 1977, P.1253). Geochemical data support the tholeiitic affinity of this dyke (Wenmenga, 1986, P.267) The coexistence of augite and orthopyroxene led to the application of Lindsley (1983, P.487) geothermometer under one atmosphere conditions in order to estimate the temperature of crystallization. This has been estimated between 1000 to 1150°C in the fine and medium grained dolerite and between 800 to 900°C in the rapid cooled chilled dolerites (Fig.12).

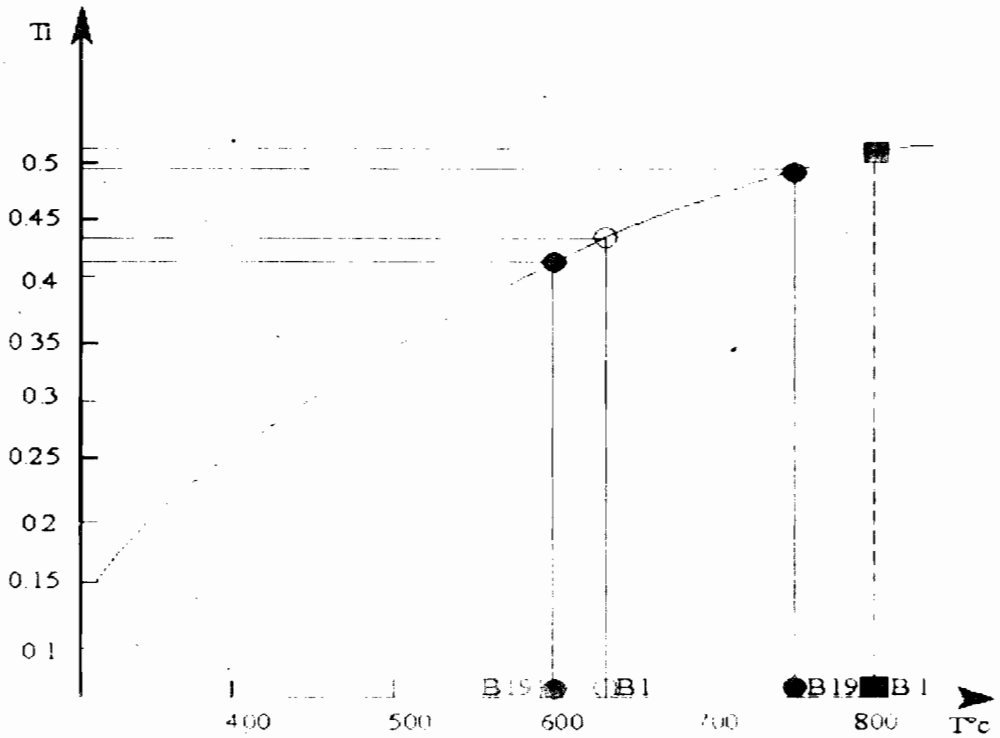

Figure 11: Discrimination diagram using Ti versus Alt composition of clinopyroxene (Leterrier and al 1982) showing dominant tholeiitic affinity of dolerites and calc-alkaline affinity of gabbros. Same legend as figure 10

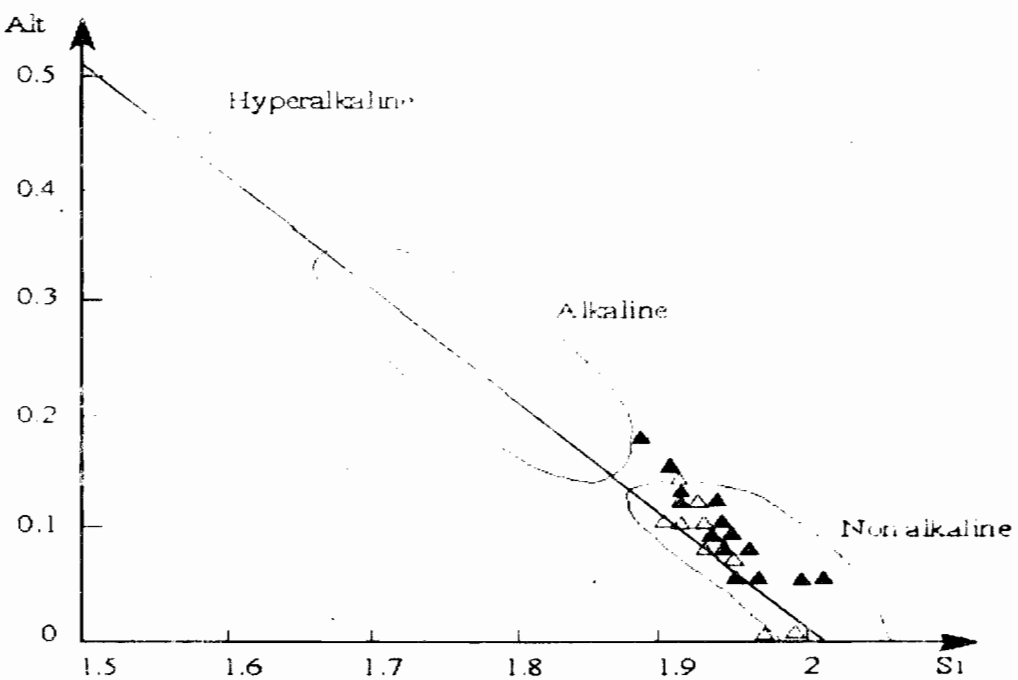

Figure 12: Coexisting augite- orthopyroxene thermometry using Di- En- Hd- Fs quadrilateral of Lindsley (1983) Full square : chilled dolerite ; full triangle and full circle : medium grained dolerite.

Similar results on the geothermometry of coexistent augite and pigeonite yielded similar temperatures between 1100° to 1150°C in Triassic dolerites (Azambre et al.,1987, P.388), 1100° to 1000°C in some Proterozoic dykes (Sutcliffe, 1989, P.71) and 900 to 1100°C in Tertiary dolerites of the south- west Greenland (Hall and al., 1988, P.705) and 900 to 1000° C in Paleozoic basaltic lavas (Pemberton and Offler, 1985, P.598). The crystallization temperature of biotite using Le Bell (1979) thermometry (Fig.13) is estimated between 600 and 750°C in the medium grained dolerites and approximately 800°C in the pegmatites. This range of temperature indicates a late magmatic crystallization of biotite. In the Sirba valley dolerite close to western Niger, Ama Salah, (1991, P.211) using the same geothermometer, obtained similar temperatures (580 to 780°C) from biotite and as well as ilmenite and titano-magnetite geothermometers. A large majority of clinopyroxenes composition representing the various bodies of the dyke, plotted in the anorogenic basalts field (Fig.14) related to crustal distension zones. The Boussouma dyke displays the same geotectonic setting as the Sirba dolerite dyke (Ama Salah, 1991, PP.204-218). Both could belong to the same distension and basic magmatic cycle, emplaced during Mesoproterozoic period (Ama Salah, 1991, P. 224) in west Africa.

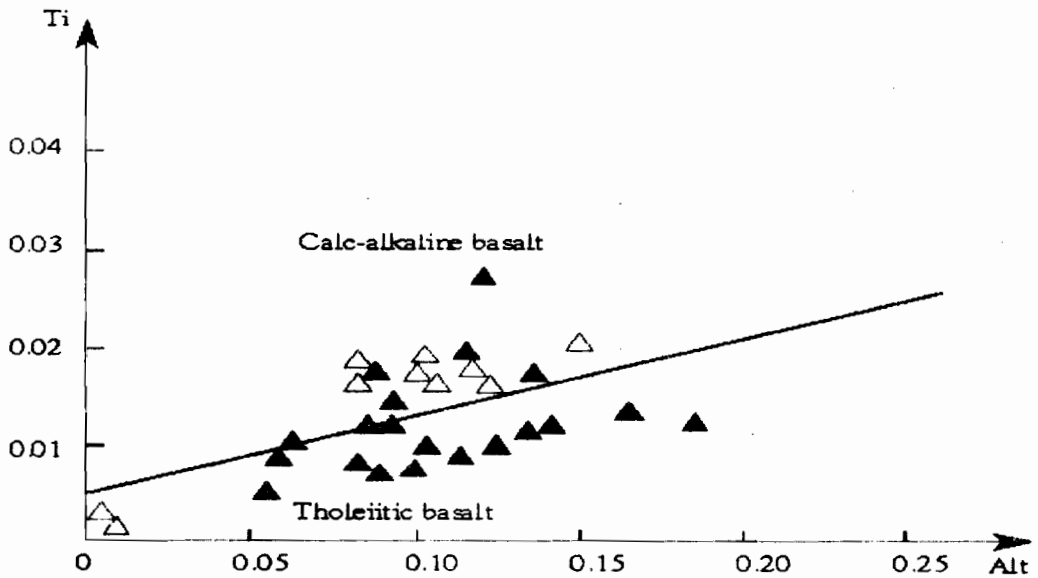

Figure 13 Crystallization temperature estimation of biotite in the basic rocks of the dyke after Le Bell, (1979). Full circle and empty circle : medium grained dolerite (B1, B19); full square : pegmatites (B'1).

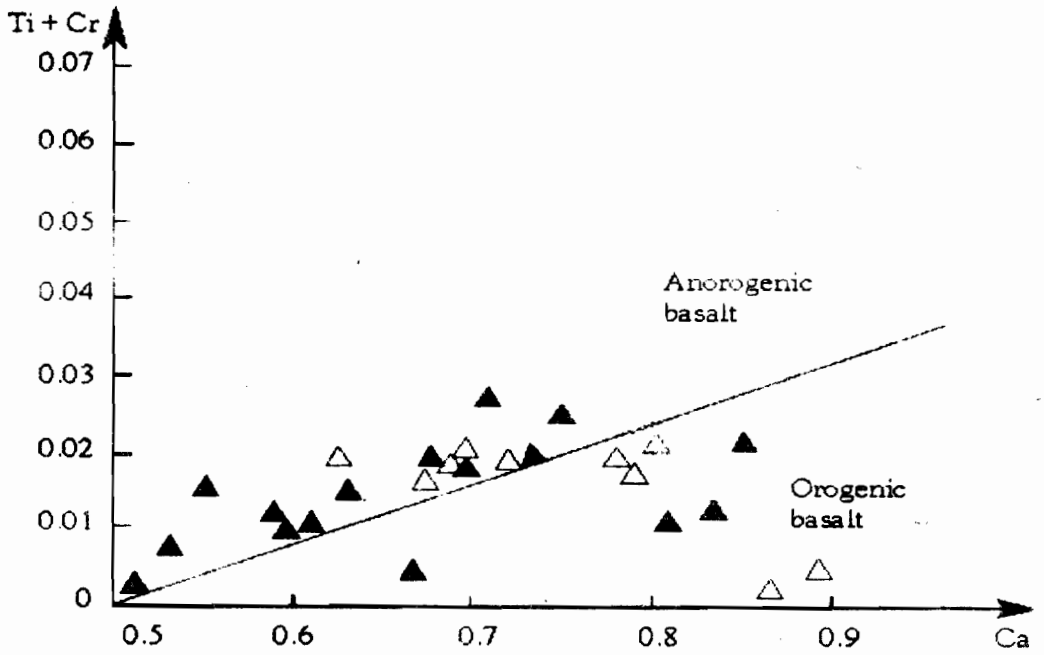

Figure 14: Clinopyroxene composition of representative rocks of Boussouma dyke, straddling the boundary between extensional and orogenic field (Leterrier and al., 1982) and showing nevertheless predominant anorogenic basalt affinity.

DISCUSSION

Boussouma dyke results from the crystallization of a tholeiitic magma saturated in water during the cooling process, which explains the constant coexistence of various anhydrous and hydrous minerals in the three main bodies of this intrusion. Silica saturation of the parental magma supports the persistence of quartz in all bodies even in olivine- bearing dolerite and gabbro. The increase in quartz content with the corresponding enrichment of Fe- clinopyroxenes and of Fe-Ti opaques from the margin to the centre of the dyke, are compatible with the process of magmatic fractionation. Major elements composition of pyroxenes is in support of the tholeiitic affinity and emplacement of the dyke in a non-orogenic setting along regional fractures. Crystallization temperatures of the melt using two pyroxenes geothermometer (1000-1150°C) corresponds to that of basaltic magmas. Temperatures provided by the biotite composition and geothermometer (750-600°C), could represent those of the final magmatic crystallization stage. Such thermal conditions of crystallization have been reported in Mesoproterozoic dolerites in Niger Republic, which are similar to Boussouma dyke in mineralogical and geochemical composition as well as in their geotectonic setting.

CONCLUSION

Field, macroscopic and microscopic observations supported by qualitative microprobe analysis have led to the identification of a petrographic suite with regular and continuous grain variation, from the margin to the core within the Boussouma dolerite dyke. This textural variation is interpreted as a result of various cooling rates and consequently to magmatic differentiation at the scale of the dyke. This cooling remained slow as expressed by the development of coronas texture in the chilled bodies. The increase of quartz and micropegmatite content and that of Fe-Ti oxides from the earlier phases (chilled dolerite, dolerite (ss), gabbro) to the evolved phases (Pegmatites), is attributed to a magmatic fractionation process. The Fe-rich composition of olivine and augite and the enrichment in ilmenite and quartz of the residual liquid are typical of tholeiitic magmas. The tholeiitic affinity related to the emplacement of the dyke in an anorogenic setting and crustal distension is further confirmed by major and minor elements composition of the clinopyroxenes and their hosted rocks. Enrichment influids of the residual liquid, generates important vapour pressure favourable to hydrated minerals crystallization as brownish to greenish hornblende and brown biotite. Two pyroxenes geothermometer indicates early temperature of magma crystallization ranging from 1000 to 1150°C and about 600 and 800°C during magmatic cooling as revealed by biotite thermometry. The excess hydrothermal fluids drawn by cracks within the magmatic mineral phases led to the formation of altered bodies in the dyke.

ACKNOWLEDGEMENTS

The authors are grateful to Michele VESCHAMBRE of the Laboratory " Magmas et Volcans " of Clermont Ferrand/France for providing graciously, microprobe analysis.

REFERENCES

Airo, M-L., 1999. Magnetic and compositional variations in Proterozoic mafic dykes in Finland, northern Fennoscandian shield. Canadian Journal of Earth Sciences, 36:891-903.

Ama Salah, I., 1991. Pétrographie et relation structurales des formations métavolcaniques et sédimentaires du Birimien du Niger occidental. Problème de l'accrétion crustale au Protérozoïque inférieur. Thèse, Université d'Orléans, Orléans, France 231 PP.

Azambre, B., Rossy, M. et Lago, M., 1987. Caractéristiques pétrologiques des dolérites tholéiitiques d'âge Triasique (ophites) du domaine pyrénéen. Bulletin de Minéralogie 110 : 379-396.

Bertrand, H., 1987. Le magmatisme tholeiitique continental de la marge ibérique, précurseur de l'ouverture de l'Atlantique central. Les dolérites du dyke de Messejana- Plasencia (Portugal-Espagne). Comptes Rendus Académiques des Sciences de Paris 304 (II, 6) : 215-220

Bickford, M.E., 1963. Petrology and structure of layered gabbro, Pleasant Bay, Maine. Journal of Geology 71 (2): 215-237.

Botha, B. J. V and Hodgson, F. D. I., 1976. Karoo dolerites in Northwestern Damaraland. Transactions Geological Society of South Africa 79: 186-190.

Cadman, A., Tarney, J and Park, R.G., 1990. Intrusion and crystallization features in Proterozoic dyke swarms In parker, Rickwood Tucker (Editors), Mafic dykes and emplacement mechanism. Balkema, Rotterdam PP.325-334.

Castaing, C., Billa, M , Milesi, J.P., Thieblemont, D., Le Metour, J., Egal, E., Donzeau, M., Guerrot, C., Cocherie, A., Chevremont, P , Tegyey, M., Itard, Y., Zida, B., Ouedraogo, I , Kote, S., Kabore, B.E., Ouedraogo, C., Ki, J.C et Zunino, C., 2003. Notice explicative de la carte géologique et minière du Burkina Faso à 1/1. 000.000. Projet "SYSMIN" n°7 ACP.BK 074UE, 3e édition, 134 PP.

El Aouli, E. H., Gasquet, D et Ikenne, M., 2001. Le magmatisme basique de la boutonnière d'Igherm (Anti- Atlas occidental Maroc) un jalon des distensions néoprotérozoiques sur la bordure nord du craton Ouest- Africain. Bulletin de la Société Géologique de France 172 (3) 309-317.

Fabries, J., Conquere, F and Arnaud, G., 1984. The mafic silicates in the Saint Quay- Portrieux gabbro-diorite intrusion crystallization conditions of a calc-alkaline pluton.. Bulletin de Minéralogie 107: 715-736

Fodor, R.V., Keil, K. and Bunch, T.E., 1975. Contribution to the mineral chemistry of Hawaiian rocks. Contribution to Mineralogy and Petrology 50: 173-195.

Fonteilles, M. et Muffat, S., 1970. Etude pétrographique de deux dolérites (ophites) à pigeonite et olivine des pyrenées occidentales. Bulletin de la Société Française de Minéralogie et de Cristallographie 93 : 555-570.

Foster, M.D., 1960. Interpretation of the composition of trioctahedral micas. Geological Survey Professional Paper 354B: 11-49.

Gamsonré, P.E., 1975. Contribution à l'étude géologique des formations précambriennes de la région de Ouahigouya (Haute Volta). Thèse, Doctorat es sciences, Université de Besançon, Besançon, France, 181 PP.

Hafid, M.A., 1992. Granites et dolérites protérozoïques de la boutonnière d'Irhem (Anti Atlas Occidental, Maroc) Pétrologie, géochimie et signification géodynamique. Thèse, Université Paris VI, Paris, France , 234 pp.

Hall, R.P.; Hughes, D.J.and Joyner, L., 1988. Complex pyroxene assemblages of Proterozoic dolerites, SE Greenland. Mineralogical Magazine 52: 703-705.

Hey, H., 1954. A new review of chlorites. Mineralogical Magazine 30: 277-292.

Kushiro, I., 1960. Si- Al relation in clinopyroxene from igneous rocks. American Journal of Sciences 258: 548-554.

Leake, B.E., 1965. The relation between tetrahedral aluminium and the maximum possible octahedral aluminium in natural calciferous amphiboles. American Mineralogists 50: 843-851.

Leake, B. E., 1978. Nomenclature of amphiboles. Canadian Mineralogist. 16: 501-520

Le Bell, L., 1979. Hydrothermal and magmatic micas within Cerrover de Santa Rosa, Perou Porphyry copper. Bulletin de Minéralogie 102: 35.41.

Leterrier, J., Maury, R.C., Thonon, P., Girard, D. and Marchal, M., 1982. Clinopyroxene composition as a method of identification of magmatic affinities of paleo- volcanic series. Earth and Planetary Sciences Letters 59: 139-154.

Lindsley, D.H., 1983. Pyroxene thermometry. American Mineralogist 68: 477-493.

Machairas, G., 1975. Le cuivre natif et les sulfures dans certaines dolérites. Bulletin de la Société française de Minéralogie et de Cristallographie 98 : 194-198

Molard, J. P., Maury, R. C., Leterrier, J. et Bourgeois, J., 1983. Teneurs en chrome et titane des clinopyroxènes calciques des basaltes: Application a l'identification des affinités magmatiques de roches paléovolcaniques. Comptes Rendus Académiques des Sciences de Paris 296 (II) : 903-908.

Mongkoltip, P. and Ashworth, J.R., 1983. Quantitative estimation of an open system symplectite forming reaction: Restricted diffusion of Al and Si in coronas around olivine. Journal of Petrology 54-(4): 635-661.

Napon, S., 1988. Le gisement d'amas sulfuré (Zn, Ag) de Perkoa dans la province du Sangyé/ Burkina Faso-Afrique de l'Ouest/ Cartographie- Etude Pétrographique, Géochimique et Métallogénique. Thèse, Université- Franche comté, Besançon, France, 275P.

Paterson, Grant et Watson Ltd., 1985. Interprétation du levé magnétique et du levé radiométrique du rayon Gamma, région d'Autorité du Liptako Gourma, Afrique Occidentale BUMIGE B Rapp. A.C.D.I (I) 377 pp.

Pemberton, J. W. and Offler, R., 1985. Significance of Clinopyroxene compositions from the Cudgegong volcanics and Toolamanang volcanics; Cudgegong- Mudgee district, NSW Australia. Mineralogical Magazine 49: 591-599.

Poidevin, J. L., 1977. Mise en évidence d'une série de tholeiites à pigeonite dans le Précambrien supérieur de la république centrafricaine. Relation avec la tectonique. Comptes Rendus Académiques des Sciences de Paris 284 : 1251-1254.

Poldervaart, A. and Hess, H.H., 1951. Pyroxenes in the crystallization of basaltic magma Journal of Geology 59: 472-489.

Pons, J., 1982. Un modèle d'évolution de complexes plutoniques: Gabbros et granitoïdes de la Sierra Morena occidentale (Espagne). Thèse, Doctorat es sciences, université Paul Sabatier, Toulouse, France, 451 PP.

Potdevin, J-L., Goffette, O. et Santallier, D., 1994. Les différences minéralogiques, chimiques et texturales entre cœur et bordures du filon de diabase de la Grande commune (Massif de Rocroi, Ardenne) des marqueurs d'un épisode d'infiltration par un fluide à CO_2 et H_2O lors d'un métamorphisme varisque synschisteux en faciès schiste vert. Bulletin de la Société géologique de France 165 (3) : 249-260

Rathna, K., Vijaya Kumar K and Ratnakar, J 2000 Petrology of the dykes of Ravipadu, Prakasam province, Andhra Pradesh, India Journal Geological Society of India 55 399-412

Reid, D.L., 1990. The Cape Peninsula dolerite dyke swarm, South Africa., In Parker, Rickwood and Tucker (Editors). Mafic dykes and emplacement mechanism, Balkema, Rotterdam.: pp. 325-334.

Reynolds, I. M., 1983. The iron- titanium oxide mineralogy of Karoo dolerite in the Eastern Cape and Southern Orange free state. Transactions Geological Society of South Africa 86: 211-220.

Rivers, T. and Mengel, F.C., 1988. Contrasting assemblages and petrogenetic evolution of corona and non corona gabbros in the Greenville province of Western Labrador. Canadian Journal of Earth Sciences 25: 1629-1648.

Ross, M. E., 1983. Chemical and mineralogic variations within four dikes of Columbia river basalt group, southeastern Columbia Plateau. Geological Society of America Bulletin 94: 1117-1126.

Ross, M. E., 1986. Flow differentiation, phenocryst alignement and compositional trends within a dolerite dike at rockport, Massachusetts. Geological Society of America Bulletin 97: 232-240.

Sawadogo, J., 1983.Etude géologique du sillon Birimien de Yalogo dans la région de Gangaol Nord de la Haute Volta. Thèse, 3e cycle, Université Franche Comté, France, 165 PP.

Somda, N.A., 1995. Etude pétrographique, géochimique et structurale des formations de Gose, au sein du Permis de recherche et d'exploitation minière d'Essakane (Sillon de Dori- Burkina Faso) Mémoire DGP, Université Blaise PASCAL, Clermont Ferrand, France, 95 PP.

Sutcliffe, R.H., 1989. Mineral variation in Proterozoic diabase sills and dykes at lake Nipigon, Ontario. Canadian Mineralogist. 27: 67-79.

Vicat, J.P. et Vellutini, P.J., 1987. Sur la nature et la signification des dolérites du Bassin Précambrien de Sembe- Ouesso (République du Congo). Precambrian Research 37 : 57-69.

Vicat, J.P. et Pouclet, A., 1995 : Nature du magmatisme lié à une extension pré- panafricaine. Les dolérites des bassins de Comba et de Sembe-Ouesso (Congo). Bulletin de la Société géologique de France 166, (4) : 355-364.

Wenmenga, U., 1986. Pétrologie des ensembles lithologiques du Protérozoïque Inférieur au Nord est de Ouagadougou (Burkina Faso, craton Ouest Africain). Etude pétrographique, géochimique et géochronologique. Thèse, Université Blaise PASCAL. Clermont Ferrand, France 275 P P.